

# Synthesis of Mg-Ti alloy by mechanical alloying

G. LIANG\*, R. SCHULZ

HERA Hydrogen Storage System, Inc., 577 Le Breton, Longueuil, Quebec, Canada J4G 1R9

E-mail: gl@herahydrogen.com

Mg-based Mg-Ti binary alloys have been synthesized by mechanical alloying of Mg and Ti powder blends. It was found that mechanical alloying of Mg and Ti results in a nanocrystalline Mg-Ti alloy and an extended solubility of Ti in Mg, due to the favorable size factor and the isomorphous structure of Mg and Ti. In the case of Mg-20at.%Ti, about 12.5% Ti is dissolved in the Mg lattice when the mechanical alloying process reaches a stable state. The rest (about 7.5 at.%) remains as fine particles in the size of 50–150 nm in diameter. Dissolution of 12.5 at.% Ti in the Mg lattice causes a contraction of the unit cell volume from 0.0464 to 0.0442 nm<sup>3</sup> and a decrease of the c/a ratio from 1.624 to 1.612 of the hexagonal structure. The supersaturated solid solution Mg-Ti alloy decomposes upon thermal annealing at temperatures above 200°C. Hydrogenation enhances the decomposition process at lower temperatures. © 2003 Kluwer Academic Publishers

## 1. Introduction

Mg-based alloys are attractive materials for hydrogen storage and for structural applications because of the low density of Mg. Tailoring the property of magnesium by forming new alloys or new structures has been the main focus for a number of researches [1–4].

Titanium has a melting point that greatly exceeds the boiling point of magnesium and therefore, alloying of Mg and Ti by conventional methods is extremely difficult. Secondly, the solubility of Ti in liquid Mg is very low [5], therefore, it is very difficult to extend the solubility of Ti in Mg by rapid solidification. Physical vapor deposition (PVD) was used to synthesize Mg-Ti alloys and the solubility of Ti in Mg phase was extended to 22.7 wt% [6].

Mechanical alloying (MA) has been proved to be an excellent technique for extending terminal solid solubility [7, 8]. The solid solubility enhancement during this non-equilibrium process can be so high that a single solid solution phase can be formed even in some immiscible systems such as Fe-Cu [9] and Cu-Co [10]. Our previous work showed that mechanically alloying of Mg-5at.% Ti results in a dissolution of Ti in Mg [11]. In this work, we extend the investigation to higher Ti content.

## 2. Experimental

Commercial grade titanium powder with a purity greater than 99% and Mg powder (>99.8% pure) were used as starting materials. Mechanical alloying was performed on a Spex 8000 ball mill in a steel milling vial under the protection of argon. The milling balls were made of stainless steel. The ball to powder mass ratio was 10:1. A small amount of powder was removed at

regular intervals for monitoring the structural changes. All the handlings were performed in a glove box under argon. Thermal annealing was performed in a hydrogen gas titration system (an automated Sievert's type apparatus) under a vacuum of 10<sup>-4</sup> torr. The hydrogen sorption properties were also evaluated by using this system.

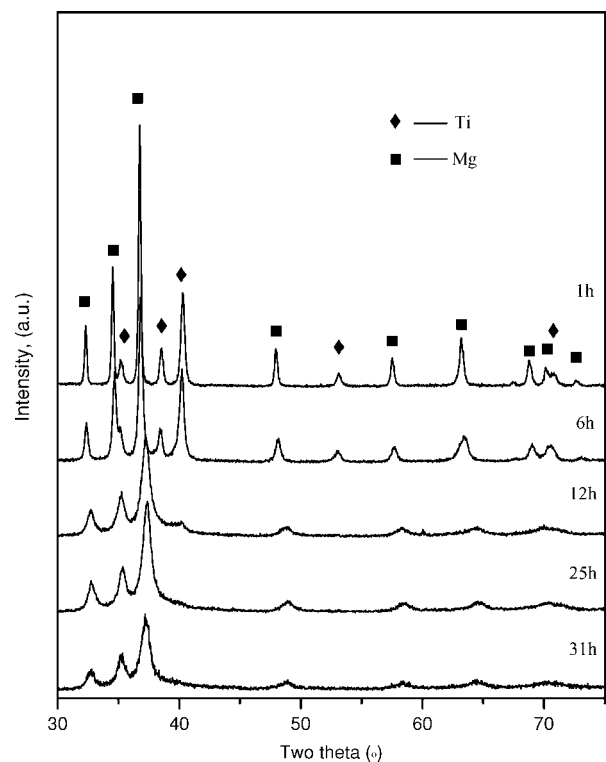


Figure 1 XRD spectra of the Mg-20at.%Ti mechanically alloyed for various times.

\* Author to whom all correspondence should be addressed.

The X-ray powder diffraction (XRD) was carried out by using Siemens D-500 diffractometer with Cu  $K\alpha$  radiation. The peak position and the instrumental broadening was calibrated by using strain free pure Si powders. The grain size was determined from X-ray line broadening by using the Williamson-Hall method, and the lattice parameters were determined from the diffraction peak positions [12].

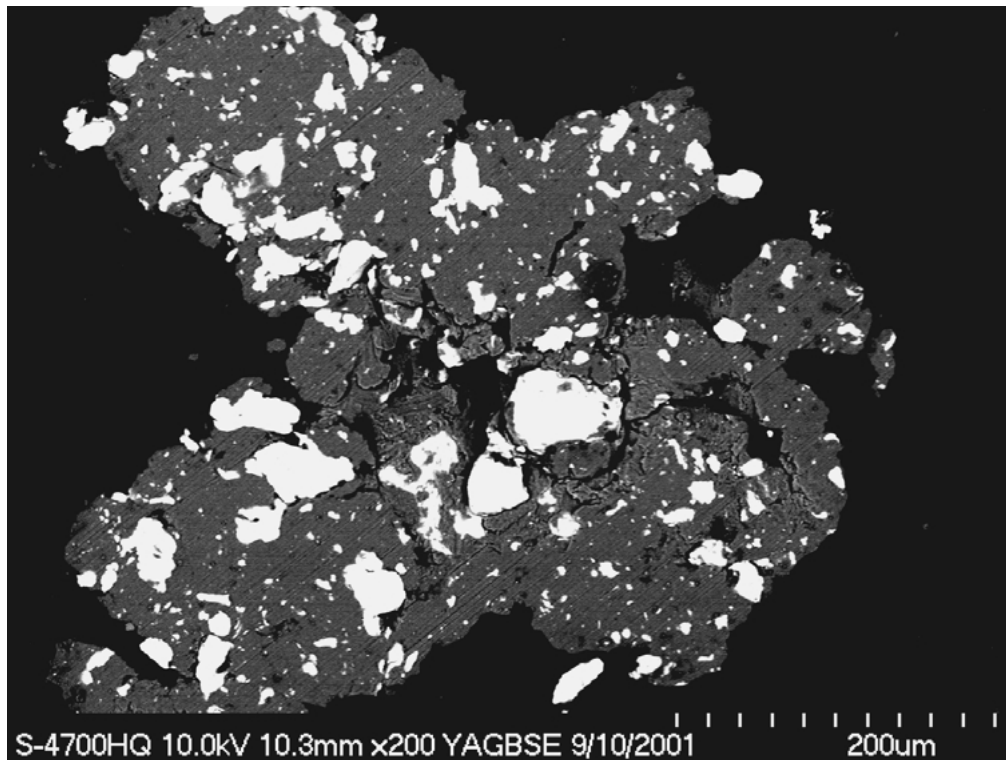
The DSC (differential scanning calorimetry) measurements were performed on a Perkin-Elmer DSC7

apparatus under the protection of argon. Field emission scanning electron micrographs were taken on a Hitachi model S4700.

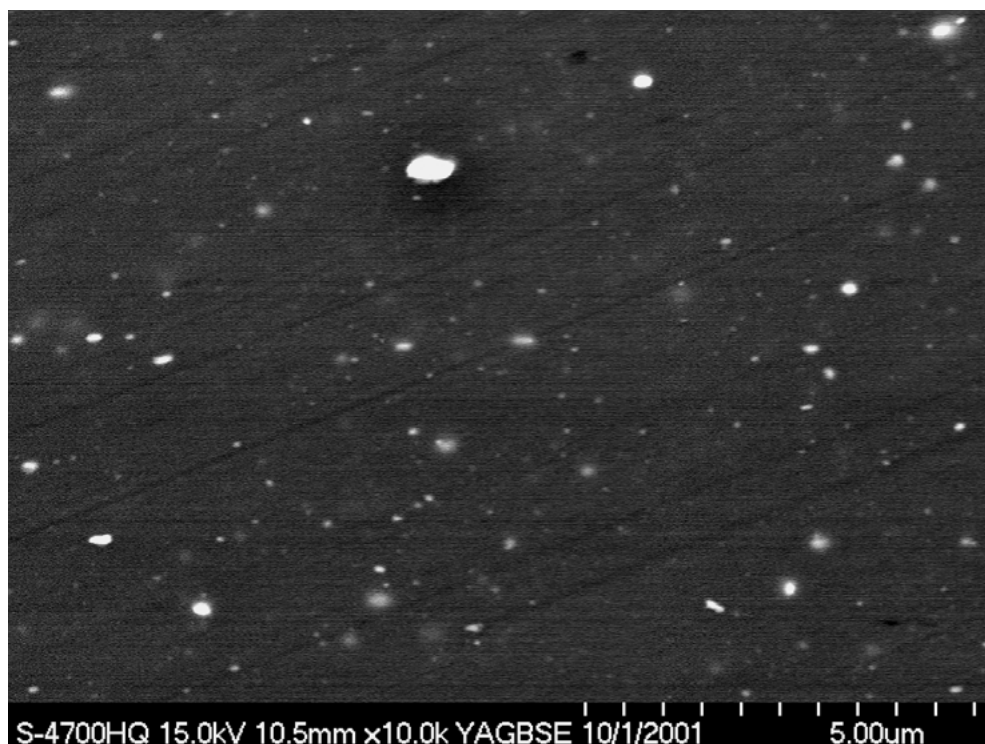
### 3. Results and discussion

#### 3.1. Mechanical alloying

Fig. 1 shows the XRD spectra of the Mg-20at.%Ti mechanically alloyed for various times. After 1 h of milling, the diffraction peaks of the Ti and Mg phases



(a)



(b)

Figure 2 Backscattered images of the Mg-20at.%Ti mechanically alloyed for 1 (a) and 31 hours (b).

can be clearly seen. The diffraction peaks of both phases become broader with increasing milling time. We observe a decrease of the diffraction intensities of the Ti phase and a concomitant peak shift of the Mg phase. After 25 hours of milling, no clear Ti peaks can be observed. This indicates that alloying between Mg and Ti has occurred, and that the Ti atoms have been dissolved in the Mg lattice.

Although the Ti peaks disappear on the XRD spectra after a long time of milling, it does not mean that all the Ti atoms have been dissolved in the Mg lattice at the atomic level. Fig. 2 shows the backscattered images of the Mg-20at.%Ti alloy after 1 and 31 hours of milling. The Ti particles have been kneaded into the Mg matrix after 1 h of milling. Most of the Ti is dissolved in the Mg lattice after 31 hours of milling, however, some fine Ti particles of 50–150 nm in diameter are still present.

Fig. 3 shows the lattice parameters of Mg in the Mg-10at.%Ti and Mg-20at.%Ti alloys as a function of milling time. Both lattice parameters  $a$  and  $c$  of the hexagonal Mg decrease with milling time owing to the dissolution of small Ti atoms in the Mg lattice. For Mg-10at.%Ti, the lattice parameters reach stable values of  $a = 0.3177 \pm 0.0002$  nm and  $c = 0.5143 \pm 0.0003$  nm after 15 hours of milling. Increasing the milling time to 40 hours does not change the lattice parameters further. For Mg-20at.%Ti, the saturated values for  $a$  and  $c$  are  $0.3161 \pm 0.0003$  nm and  $0.5097 \pm 0.0002$  nm respectively after 12 hours of milling. The evolution of the lattice parameters with milling time indicates that the alloying process has been completed after about 15–25 hours of milling for both samples. The  $c/a$  ratio of the hexagonal Mg changes from 1.624 to 1.618 in the Mg-10at.% alloy and to 1.612 in the Mg-20at.%Ti alloy.

The lattice parameters of Mg are plotted as a function of Ti content for the Mg-Ti alloys made by PVD [6] and for the Mg-Ti alloys made by mechanical alloying (this work) in Fig. 4. Based on the relationship

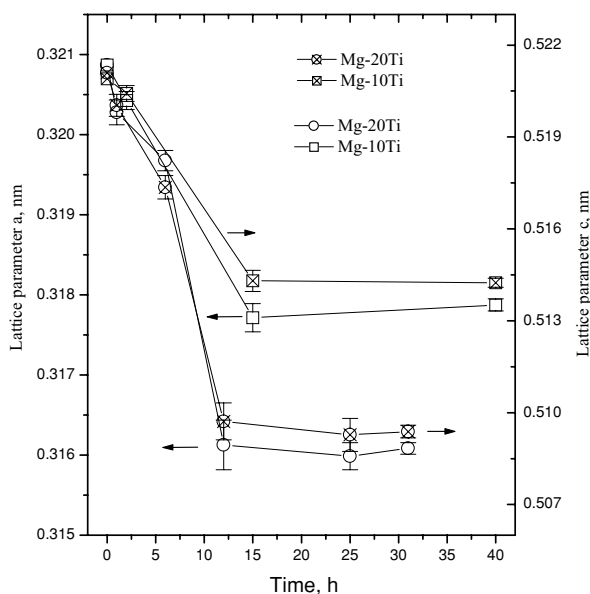


Figure 3 Variation of lattice parameters as a function of milling time.

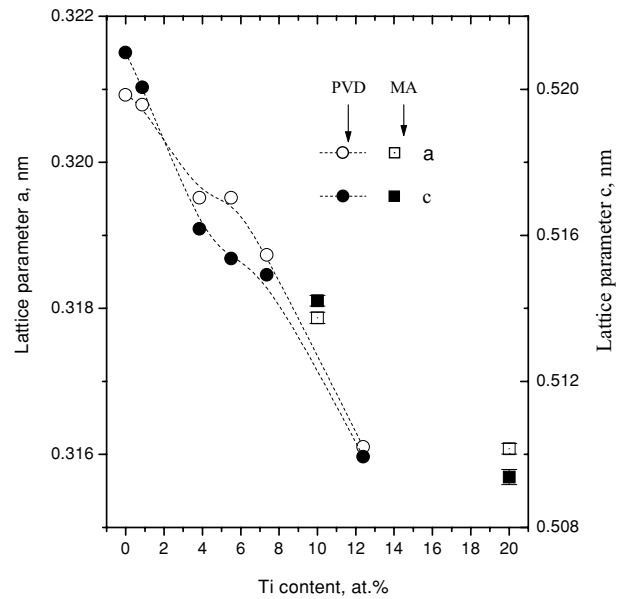


Figure 4 Relationship of the lattice parameters of the hexagonal Mg in the Mg-Ti alloy with Ti content.

of the lattice parameters with Ti content, we estimate that about 8 at.%Ti in the Mg-10Ti and 12.5 at.% of Ti in the Mg-20Ti are dissolved in Mg to form a solid solution when the mechanical alloying reaches a stable state.

When we inspect the X-ray spectra in Fig. 1 carefully, we can observe a small broad Ti peak at about  $40^\circ$  in the Mg-20at.%Ti alloy after 12 hours of milling. Increasing the milling time to 25 and 31 hours, this small peak is buried in the high background. As pointed out previously, ordinary X-ray diffraction is not sensitive to crystals smaller than several nanometers embedded in a matrix, especially, when the grain size is very small and the background is high [13, 14].

Fig. 5 shows the variation of the crystallite size and the microstrain of Mg as a function of milling time. The crystallite size decreases and reaches about 35 nm after 25 hours of mechanical alloying. In the mean time, the microstrain increases and reach 0.7%. Further increase of milling time does not lead to additional change of crystallite size and microstrain.

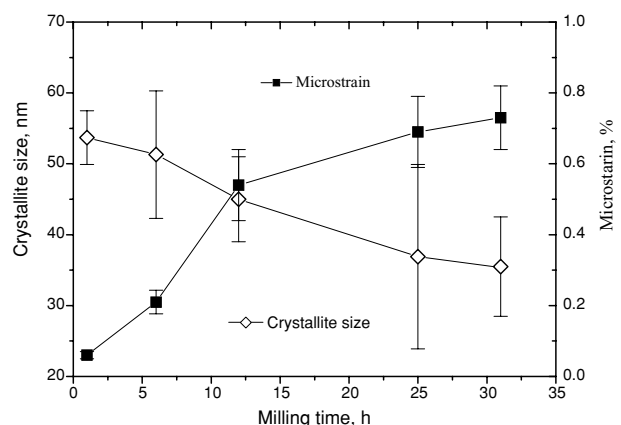


Figure 5 Variation of crystallite size and microstrain with milling time.

### 3.2. Decomposition upon thermal annealing treatment

The nanostructure, extended solubility and the reduced  $c/a$  ratio of the mechanically alloyed Mg-Ti may lead to novel mechanical and hydrogen storage properties. However, the metastable structure of the supersaturated Mg(Ti) tends to vanish upon exposure to high temperatures. It is of significance to know the thermal stability of the nanocrystalline Mg(Ti) supersaturated solid solutions.

Fig. 6 shows the XRD spectra of the mechanically alloyed Mg-20at.%Ti after 1 hour of annealing at various temperatures. There is no obvious change in the diffraction pattern and the peak positions after 1 h of annealing at temperatures below 200°C. The Ti peaks start to show up after annealing at 300°C (not shown), and become stronger at 350°C. The diffraction peaks of both Mg and Ti phases are broad after annealing at 350°C, indicating that the grain growth is slow below this temperature.

The variation of the crystallite size and microstrain with annealing temperature is shown in Fig. 7. There

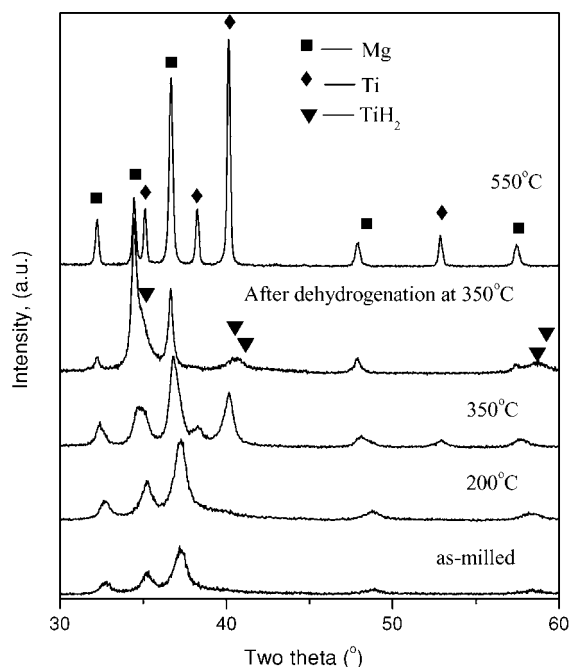


Figure 6 XRD spectra of the Mg-20at.%Ti after 1 h of annealing at various temperatures and after hydrogenation (3 days).

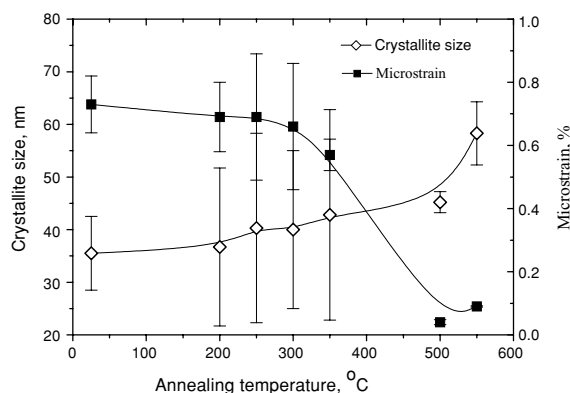


Figure 7 Variation of the crystallite size and microstrain with annealing temperatures (1 hour).

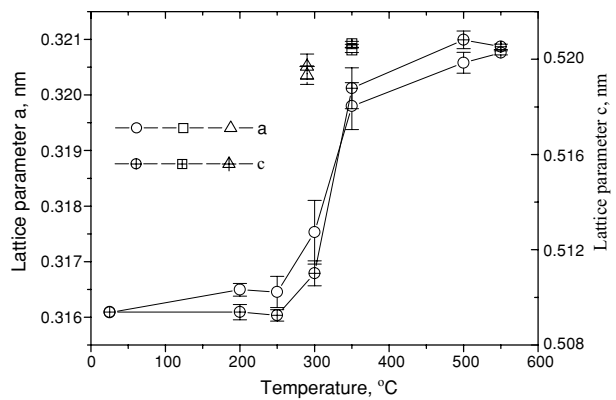


Figure 8 Variation of the lattice parameters with annealing temperatures for simple annealing of 1 h (circle); hydrogenation at 290°C for 3 days (triangle) and hydrogenation at 350°C for 3 days (square).

is not much grain growth below 500°C. The high stability of the nanocrystalline Mg-Ti alloys is probably due to the retardative effect of fine titanium particles which pin grain boundaries and thus act against grain growth. The strain release is slow below 300°C. This may be explained by pinning effects of Ti solutes on dislocations. Without Ti, the strain release is very fast at 200°C for Mg [11].

Fig. 8 shows the variation of the lattice parameters with annealing temperature. Only slight change of the lattice parameter  $a$  is observed at temperatures below 250°C. Both  $a$  and  $c$  start to increase at 300°C and reach values close to those of pure Mg at 500°C. The variation of unit cell volume is shown in Fig. 9. The unit cell volume decreases from 0.0464 to 0.0442 nm<sup>3</sup> after 25 hours of mechanical alloying, and increases back from 0.0442 to 0.0464 nm<sup>3</sup> after annealing treatment at 500°C for 1 h.

Fig. 10 shows the DSC curves of the Mg-20at.%Ti alloy after 1 and 25 hours of mechanical alloying. Two scans were conducted under the same conditions for each sample. The second run was used as baseline. The curves shown in Fig. 10 is the difference of the first run with the second run (baseline). As it can be seen, after 1 h of mechanical alloying, no obvious reaction peak is observed. However, a broad exothermic reaction

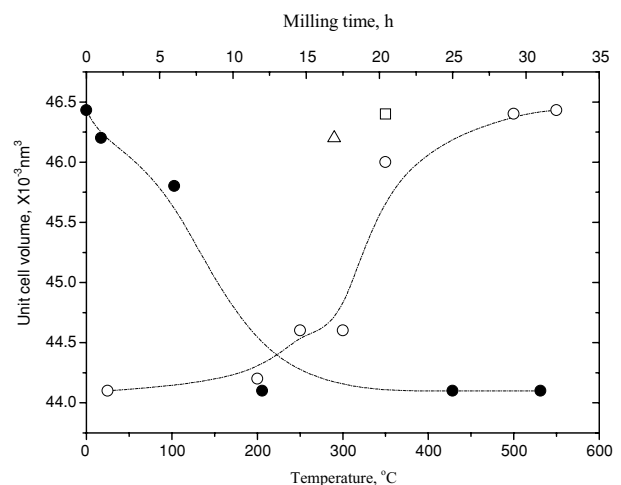


Figure 9 Variation of the unit cell volume with milling time (solid circle) and annealing temperature for thermal annealing (open circle), hydrogenation at 290°C (triangle) and hydrogenation at 350°C (square).

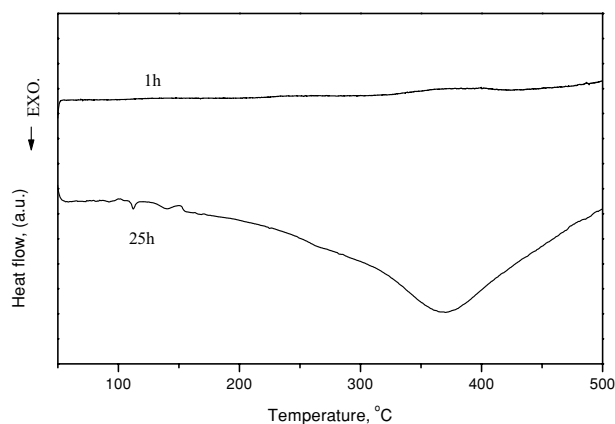


Figure 10 DSC curves of the Mg-20at.%Ti mechanically alloyed for 1 and 25 h (scan rate: 20°C/min).

starting at 120°C is observed for the sample mechanically alloyed for 25 h. This broad exothermic peak most likely results from the decomposition reaction of the supersaturated solid solution Mg-Ti alloy and the release of strain and grain boundary energies (see Fig. 7). We do not observe separate DSC peaks for different reaction.

The exothermic reaction is not complete at 500°C (since the sample starts to react with the Cu crucible above 500°C, the measurements were stopped at this temperature). The exothermic reaction takes place at very low temperature (although very slow). By integrating the peak area from 120°C to 500°C, we obtain a reaction heat of 3.8 kJ/mol. Since the strain level is not high (<0.7%) and the grain size is not very small (>35 nm), the contribution of strain energy and grain boundary energies to the heat release may not be large. We believe that the heat release mainly comes from the decomposition reaction. However, the above value is an estimation of the real reaction enthalpy because the reaction is not completed at 500°C as mentioned before. The theoretical enthalpy of formation for the Mg-20at.%Ti alloy is about +10 kJ/mol [15].

Using Kissinger's method, DSC measurements under different scanning rates have been done in an attempt to obtain the apparent activation energy of the exothermic reaction, even though the validity of a Kissinger analysis in terms of a single process is not strictly fulfilled. The determination of the activation energy may help us understand the underlying process occurring during the exothermic reaction. Fig. 11 shows the Kissinger's plot of  $\ln(S/T_p^2)$  versus the reciprocal peak temperature  $T_p$ , where  $S$  is the scanning rate. From the slope, we determine an activation energy of 134.1 kJ/mol for this exothermic reaction process. This value is close to the activation energy of the self-diffusion of Mg [16]. It may indicate that the exothermic reaction is dominated by a decomposition reaction of the supersaturated solid solution controlled by the self-diffusion of Mg. There is no data available for the diffusion of Ti in Mg, therefore, we can not confirm such a hypothesis.

### 3.3. Effect of hydrogenation

The mechanically alloyed Mg-Ti alloy powders can be easily activated at 290°C under 10 bars of hydrogen.

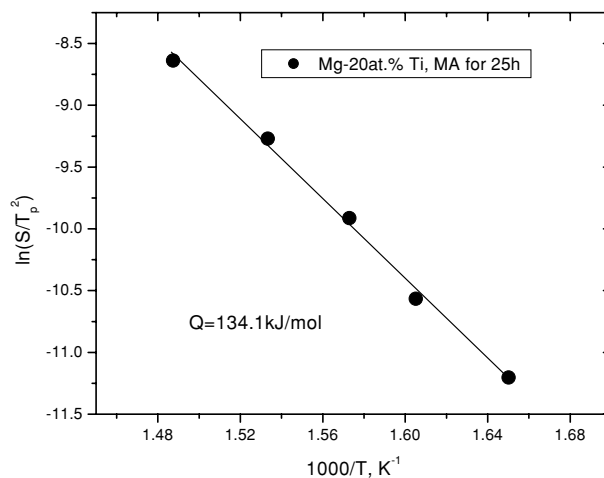


Figure 11 Kissinger plot of scanning rate ( $S$ ) versus peak temperature ( $T_p$ ).

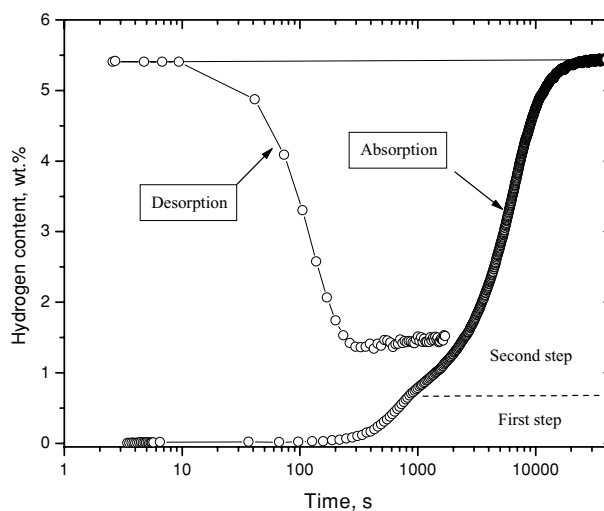


Figure 12 First hydrogen absorption/desorption curves of the Mg-20at.%Ti mechanically alloyed for 31 h (at 290°C under 10 bars).

We observe two clear steps on the hydrogen absorption curve of the Mg-20at.%Ti alloy shown in Fig. 12. In the first step, a fast hydrogen absorption takes place, and 0.7wt.% of hydrogen has been absorbed. This absorption results from the formation of  $TiH_2$  of the free Ti which is present in the mechanically alloyed sample. After that a slow hydrogen absorption reaction due to the hydrogenation of the supersaturated Mg(Ti) solid solution occurs. The hydrogen desorption is fast, however, the amount of hydrogen desorbed is 1.4 wt% short comparing with that of absorption. This discrepancy is equivalent to the amount of hydrogen in  $TiH_2$  which can not be desorbed.

X-ray analysis shows that hydrogenation causes a decomposition of the Mg(Ti) solid solution into  $MgH_2$  and  $TiH_2$  (see Fig. 6). The  $TiH_2$  stays as hydride after hydrogen desorption at 350°C under moderate vacuum. The lattice parameters of Mg after hydrogen desorption are shown in Fig. 8. In comparison with the data obtained after simple thermal annealing, we observe that hydrogenation enhances the decomposition of the supersaturated Mg-Ti alloy at low temperatures. The lattice parameters of Mg after hydrogen absorption/desorption at

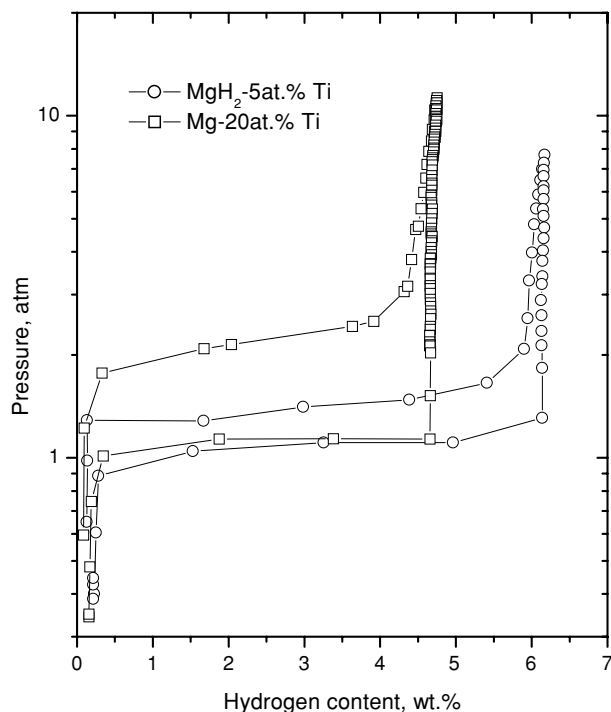


Figure 13 PCT curves of the mechanically alloyed Mg-20at.%Ti and the mechanically milled MgH<sub>2</sub>-5at.%Ti at 290°C.

290°C are close to those of pure Mg. However, some Ti may remain in the Mg lattice. Ti solutes may cause high hysteresis in the hydrogen sorption as shown in Fig. 13. We observe that the hydrogen absorption plateau pressure is much higher for the Mg-20at.%Ti in comparison to that of the Mg-5at.%TiH<sub>2</sub> made by mechanical grinding [17], while their desorption plateau pressures are basically the same. No destabilization of the magnesium hydride by adding Ti is achieved.

#### 4. Conclusions

1. Mechanical alloying of Mg and Ti powder mixtures leads to a solid solution of Ti in Mg. Some free Ti still remains when the mechanical alloying process reaches stable state. Dissolution of Ti in Mg causes a lattice contraction.

2. The supersaturated Mg(Ti) solid solution is relatively stable at temperatures below 250°C. Phase decomposition becomes fast at 300°C.

3. Hydrogenation accelerates the phase decomposition. The Mg(Ti) solid solution transforms to MgH<sub>2</sub> and TiH<sub>2</sub> upon hydrogen sorption. Due to such decomposition, no destabilization of the MgH<sub>2</sub> is achieved.

#### References

1. D. L. DOUGLASS, in Proc. Int. Symp. On Hydrides for Energy Storage 9, edited by A. F. Andersen and A. J. Maeland (Pergamon, Oxford, 1978) p. 151.
2. P. SELVAM, B. VISWANATHAN, C. S. SWAMY and V. SRINIVASAN, *Int. J. Hydrogen Energy* **11** (1986) 169.
3. F. H. FROES, *Mater. Sci. Eng. A* **117** (1989) 19.
4. F. HEHMANN and H. JONES, "Magnesium Technology" compiled by C. Baker, G. W. Lorimer and W. Unsworth (Institute of Metals, London) p. 83.
5. A. A. NAYEB-HASHEMI and J. B. CLARK, "Phase Diagrams of Binary Magnesium Alloys" (ASM International, Metals Park, OH 1988).
6. C. B. BALIGA, P. TSAKIROPOULOS, S. B. DODD and K. W. GARDINER, Proc. 3rd Int. Magnesium Conf. Manchester, UK, 1996, p. 627.
7. C. C. KOCH, in Proc. of Metals and Alloys, Materials Science and Technology, edited by R. W. Cahn, Vol. 15 (VCH, Weinheim, Germany, 1991).
8. A. R. YAVARI, P. J. DESRE and T. BENAMEUR, *Phys. Rev. Lett.* **68** (1992) 2235.
9. J. ECKERT, J. C. HOLZER, C. E. KRILL and W. L. JOHNSON, *J. Mater. Res.* **7** (1992) 1751.
10. C. GENTE, M. OEHRING and R. BORMANN, *Phys. Rev. B* **48** (1993) 13244.
11. G. LIANG and R. SCHULZ, to be published.
12. H. P. KLUG and L. ALEXANDER, "X-ray Diffraction Procedures for Polycrystalline and Amorphous Materials," 2nd ed. (John Wiley & Sons, New York, 1974).
13. C. T. LEONARD and C. C. KOCH, *Scripta Mater.* **36** (1997) 41.
14. G. H. KIM, H. S. KIM and D. W. KIM, *Scripta Mater.* **34** (1996) 421.
15. F. R. DE BOER, R. BOOM, W. C. M. MATTENS, A. R. MIEDEMA and A. K. NIESSSEN, "Cohesion in Metals, Transition Metal Alloys" (North-Holland Physics, Amsterdam, 1988).
16. C. J. SMITHELLS, "Smithells Metals Reference," edited by E. A. Brandes, 6th ed. (Butterworths, London, 1983) p. 13.
17. G. LIANG, J. HUOT, S. BOILY, A. VAN NESTE and R. SCHULZ, *J. Alloy & Comp.* **292** (1999) 247.

Received 13 May

and accepted 16 October 2002